The electrical double layer in wall–wall hypernetted chain approximation with bridge functions

Phil Attard and S. J. Miklavic

Citation: The Journal of Chemical Physics **99**, 6078 (1993); doi: 10.1063/1.465905
View online: http://dx.doi.org/10.1063/1.465905
View Table of Contents: http://scitation.aip.org/content/aip/journal/jcp/99/8?ver=pdfcov
Published by the AIP Publishing

The electrical double layer in wall–wall hypernetted chain approximation with bridge functions

Phil Attard and S. J. Miklavic[a)]
Department of Physics, Faculty of Science, Australian National University, Canberra, Australian Capital Territory, 0200, Australia

(Received 5 April 1993; accepted 7 July 1993)

The wall–wall Ornstein–Zernike equation is formulated for the case of charged walls in a primitive model electrolyte. Numerical results are presented for the modified hypernetted chain (HNC) closure, which includes the effects of ion size and correlations. The bare HNC gives attractions between like-charged surfaces rather too readily, but this is ameliorated by the inclusion of the first bridge diagram. The singlet approach is shown to be accurate in divalent electrolyte, and in the large separation asymptotic regime. The method is less reliable in dilute monovalent electrolyte.

I. INTRODUCTION

The Poisson–Boltzmann theory is universally used to describe electrolytes and charged particles, even though as a mean-field aproximation it neglects the size and correlations of the ions. In consequence certain quantities, (such as the surface charge or the activity coeffcients), which are measured by fitting the theory to experimental data, become effective parameters that incorporate the errors of the approximation. For example, the degree of ion binding and the departure of the ions from ideality, are often artefacts of overestimates of the actual double layer force and of the electrolyte decay length by the mean-field approximation. These are quantitative errors, but sometimes the Poisson–Boltzmann theory can even be qualitatively wrong. For example, it fails to predict correlation attractions between like-charged surfaces, which occur in multivalent electrolytes, oscillations in the force, and ion density profiles, which occur at higher concentrations, and negative capacitances and reversal of zeta potentials, which occur at higher surface charges. These unusual effects have practical significance, such enhanced rates of flocculation and coagulation, secondary minima in particle interaction potentials, and nonmonotonic behavior of electrodes and electrophoresis cells.

Obviously it is desirable to have a more sophisticated theory than the mean-field Poisson–Boltzmann approximation to analyze experimental data. Specifically one needs to include the effects of ion size and the correlations between them. Simulations and inhomogeneous integral equations provide benchmarks to test other theories, but are themselves too intractable (i.e., the computer algorithms are lengthy and specialized, and they require advanced machines, large amounts of memory, and a lot of CPU time) to be used to fit actual experimental data. On the other hand, singlet integral equation theories do include the effects of ion size and correlations, and are relatively simple to program and to run. They are potentially a practical approach to analyzing experimental data, provided that the regime of applicability of the more approximate theory can be established. The point of this paper is to formulate a singlet integral equation theory for interacting electrical double layers, and to test it against benchmarks.

Treatments of an isolated charged wall, which have been reviewed,[1] include modifications to the Poisson–Boltzmann theory,[2] inhomogeneous integral equations,[3] and simulations.[4] The singlet Ornstein–Zernike equation,[5] is exact apart from the wall–ion closure approximation, which has included the mean spherical and the hypernetted chain. The latter has been significantly improved by the inclusion of the first bridge diagram.[6]

Interacting charged planar walls have been studied by Kjellander and Marčelja using the inhomogeneous Ornstein–Zernike equation and the hypernetted chain closure for the ion–ion correlation functions (see, e.g., Refs. 7, 8, and 9, and references therein). Both this approach and simulations[10,11] have quantitatively confirmed the existence of attractions between similarly charged surfaces in divalent electrolyte, which were originally predicted by Oosawa,[12] and which are properly considered as part of the van der Waals force.[13,14] Lozada-Cassou and co-workers have used a singlet approach to study the pressure between charged walls.[15,16] In the present work we shall be using a different singlet approach based upon the wall–wall Ornstein–Zernike equation derived by Attard *et al.*[17] Although approximate, singlet theories have the advantage that they are orders of magnitude more computationally tractable than either simulations or inhomogeneous integral equations, and they complement these more sophisticated approaches in the problematic large-separation asymptotic regime, as well as providing a basis for analytic treatments of the double layer. There are systematic procedures for improving the accuracy of the singlet appraches, and they have proved feasible for quantitative fits to experimental data.[18]

The aims of this paper are to derive the wall–wall Ornstein–Zernike equation for charged walls in an electrolyte, and to present a computational algorithm. We test the hypernetted chain closure, including the first resummed bridge diagram, against simulation and the inhomogeneous approach. Our conclusion is that the wall–wall method is

[a)]Address: Food Technology, and Physical Chemistry 2, Chemical Center, University of Lund, P.O. Box 124, S-221 00, Lund, Sweden.

 0021-9606/93/99(8)/6078/9/$6.00

viable in certain regimes (in the case of structural oscillations, and at large separations), but for dilute monovalent electrolyte at moderate to high surface charges it is less reliable than the nonlinear Poisson–Boltzmann theory. We point to possible improvements to the hypernetted chain closure to the wall–wall Ornstein–Zernike equation. In a forthcoming publication we shall explore the simpler mean spherical approximation for the bulk correlation functions,[19] and undertake an asymptotic analysis of the electrical double layer.[20]

II. ANALYSIS

A. Wall–ion

Consider a primitive model electrolyte consisting of ions of charge q_α, density ρ_α, and hard-sphere diameter d_α, in contact with a plane hard wall with surface charge density σ located at $z=-\delta$, and let the plane of closest approach of all the ions be at $z=0$. The electroneutrality condition is[1]

$$-\sigma=\sum_\gamma q_\gamma\int_{-\infty}^{\infty}\rho_\gamma(z)dz=\sum_\gamma q_\gamma\rho_\gamma\int_0^\infty H_\gamma(z)dz, \tag{2.1}$$

where the ion density profiles, $\rho_\gamma(z)=\rho_\gamma[1+H_\gamma(z)]$, vanish inside the wall, $[H_\gamma(z)=-1,\ z<0]$, $H_\gamma(z)$ is the wall–ion total correlation function, and the neutrality condition of the bulk electrolyte, $\Sigma_\gamma q_\gamma\rho_\gamma=0$, has been used. The mean electrostatic potential is

$$\psi(z)=\begin{cases}\displaystyle\sum_\alpha\frac{q_\alpha\rho_\alpha}{\epsilon_0\epsilon}\int_z^\infty H_\alpha(z')(z-z')dz' & z\geqslant 0\\ \psi(0)-\sigma z/\epsilon_0\epsilon & -\delta\leqslant z<0\\ \psi(0)+\sigma\delta/\epsilon_0\epsilon & z<-\delta\end{cases}, \tag{2.2}$$

where ϵ_0 is the dielectric permittivity of free space, and ϵ is the relative permittivity of the medium. The arbitrary constant is chosen so that the potential goes to zero in the electrolyte far from the wall; $\psi(0)$, the potential at the plane of closest approach of the ions to the wall, represents the potential drop across the double layer, and has same sign as the surface charge, at least at low coupling. The location of the plane of surface charge at $z=-\delta$ has no effect on the mean potential in the fluid.

The formally exact closure to the wall–ion Ornstein–Zernike equation is

$$\ln[1+H_\alpha(z)]=D_\alpha(z)-\beta q_\alpha\psi(z)+2\pi\sum_\gamma\rho_\gamma\int_{-\infty}^{\infty}dz'\times H_\gamma(z')\int_{|z-z'|}^\infty dr\,rc^s_{\gamma\alpha}(r),\quad z\geqslant 0. \tag{2.3}$$

Here $\beta=1/k_BT$, and

$$c^s_{\alpha\gamma}(r)=c_{\alpha\gamma}(r)+\beta q_\alpha q_\gamma/4\pi\epsilon_0\epsilon r \tag{2.4}$$

is the short-ranged part of the bulk ion–ion direct correlation function. The wall–ion bridge function is neglected in the hypernetted chain approximation

$$D_\alpha(z)=0,\quad \text{(HNC)}, \tag{2.5}$$

but it may also be approximated by the first resummed bridge diagram,[6]

$$D_\alpha(z_2)=\frac{1}{2}\sum_{\gamma\lambda}\rho_\gamma\rho_\lambda\int H_\gamma(z_3)H_\lambda(z_4)h_{\gamma\alpha}(r_{23})\times h_{\lambda\alpha}(r_{24})h_{\lambda\gamma}(r_{34})d\mathbf{r}_3\,d\mathbf{r}_4,\quad \text{(HNCl)}. \tag{2.6}$$

Here a cylindrical coordinate system is used, with $r_{23}^2=r_3^2+(z_2-z_3)^2$, and $r_{34}^2=r_3^2+r_4^2-2r_3r_4\cos\theta_{34}+(z_3-z_4)^2$. For the bulk fluid, the total (h) and direct (c) correlation functions that appear in these expressions may be calculated using standard techniques. In this work we use the hypernetted chain closure, with and without the first resummed bridge diagram.[21,22]

We shall later require the short-ranged part of the wall–ion direct correlation function,

$$C^s_\alpha(z)=C_\alpha(z)+\beta V_\alpha(z),\quad \text{all } z, \tag{2.7}$$

where the electrostatic potential is

$$V_\alpha(z)=\frac{q_\alpha\sigma}{2\epsilon_0\epsilon}(R-|z+\delta|)+\frac{q_\alpha}{2}\psi(0),\quad \text{all } z. \tag{2.8}$$

This is the potential due to walls of size R, (all physical results become independent of R in the limit $R\to\infty$), and the arbitrary constant is chosen so that $C^s_\alpha(z)\to 0$, $z\to\infty$. Note, however, that within the wall, $C^s_\alpha(z)\to$constant, $z\to-\infty$. Substitution of these definitions into the wall–ion Ornstein–Zernike equation yields

$$C^s_\alpha(z)=H_\alpha(z)+\beta q_\alpha\psi(z)-2\pi\sum_\gamma\rho_\gamma\int_{-\infty}^{\infty}dz'\,H_\gamma(z')\times\int_{|z-z'|}^\infty dr\,rc^s_{\gamma\alpha}(r),\quad \text{all } z. \tag{2.9}$$

B. Wall–wall

Attard *et al.*[17] derived the wall–wall Ornstein–Zernike equation for the interaction free energy per unit area by considering the large radius limit of two interacting solutes. Their final result is readily interpreted as the diagramatic definition of the potential of mean force per unit area applied to walls, without the need to refer to the macrosphere limit by which it was originally obtained (cf. Ref. 18). Consequently, the formally exact result for the interaction free energy per unit area between identically charged walls in an electrolyte is

$$\beta F(z)=\beta V(z)-D(z)-\sum_\gamma\rho_\gamma\int_{-\infty}^{\infty}H_\gamma(z')\times C_\gamma(z-z')dz',\quad z\geqslant 0. \tag{2.10}$$

Here wall–wall quantities lack subscripts, including the wall–wall electrostatic potential

$$V(z)=\frac{\sigma^2}{2\epsilon_0\epsilon}(R-|z+2\delta|)+\sigma\psi(0),\quad \text{all } z. \tag{2.11}$$

Again the arbitrary constant has been chosen to make the interaction free energy decay to zero at large separations,

as will shortly become evident. The bridge function can be neglected (HNC) or approximated by the first resummed bridge diagram

$$D(z)=\pi\sum_{\gamma\lambda}\rho_\gamma\rho_\lambda\int_{-\infty}^{\infty}dz_3\int_{-\infty}^{\infty}dz_4 H_\gamma(z_3)H_\gamma(z-z_3)\times H_\lambda(z_4)H_\lambda(z-z_4)\int_0^{\infty}dr\, r h_{\lambda\gamma}(r_{34}),$$

(HNCD), (2.12)

where $r_{34}^2=r^2+(z_3-z_4)^2$.

Now the wall–ion direct correlation function will be replaced by its short-ranged counterpart, Eq. (2.7). Using Eq. (2.8) one has

$$\sum_\gamma\rho_\gamma\int_{-\infty}^{\infty}H_\gamma(z')V_\gamma(z-z')dz' = \frac{-\sigma^2}{2\epsilon_0\epsilon}(R-|z+2\delta|)-\sigma\psi(0)+\sigma\psi(z+\delta),\quad \text{all } z, \tag{2.13}$$

where the electroneutrality and potential results, Eqs (2.1) and (2.2), have been used. The final result for the interaction free energy between planar walls is

$$\beta F(z)=\beta\sigma\psi(z+\delta)-D(z)-\sum_\gamma\rho_\gamma\int_{-\infty}^{\infty}H_\gamma(z')\times C_\gamma^{\sigma}(z-z')dz',\quad z\geqslant 0. \tag{2.14}$$

Note that the separation convention is such that for $z<0$ electrolyte is excluded from between the walls. The first term represents the electrostatic energy of one wall due to the electrostatic potential of the other, [the distance between the surface charges is $z+2\delta$, but recall that $\psi(z)$ is the potential a distance $z+\delta$ from the surface charge]. It can be shown explicitly that this result for the interaction free energy is independent of the location of the plane of surface charge, [the δ dependence in the mean potential cancels identically with a contribution in $C_\gamma^{\sigma}(z)$]. The functions $\psi(z)$, $H_\alpha(z)$, and $C_\alpha^{\sigma}(z)$ represent properties of an isolated wall, and hence no further iteration is required to evaluate the interaction free energy of two walls. Even though neither $H_\alpha(z)$ nor $C_\alpha^{\sigma}(z)$ decay to zero as $z\to-\infty$, it may be confirmed that the convolution integral is convergent. In fact, it is exponentially short ranged, and the bridge contribution is expected to decay twice as fast. Finally, the above analysis is for two identical walls; the generalization to two different walls is immediate and obvious.

This result for the free energy of interacting electrical double layers, which for fluids with short-ranged potentials was obtained by Attard *et al.*,[17] may be termed the singlet wall–wall Ornstein–Zernike equation, by analogy with the terminology used for an isolated wall. The HNC closure used at this level of approximation should be distinguished from the approaches where the approximation is applied to the inhomogeneous ion–ion correlation functions,[7–9] which method may be anticipated to be more accurate and more demanding. Intermediate between these two is the singlet approach of Lozada-Cassou,[15,16] who obtains the density profiles within a single solute consisting of two walls, and the pressure via the contact theorem. Henderson[23] has recently given a result similar to Eq. (2.14), but for spherical colloids rather than the planar walls considered here. Verwey and Overbeek[24] discuss the electrical double layer free energy in Poisson–Boltzmann approximation.

C. Computer algorithm

There are three main stages in the determination of the interaction free energy. First the bulk ion correlation functions are found, then the wall–ion potential and density profiles are determined, and finally the interaction free energy convolution integral is evaluated. For the case of the HNCD closure, two further substages are needed to evaluate the bulk and the wall–ion bridge functions using the current total correlation functions. These bridge functions are then used to refine the total correlation functions. Self-consistency was generally achieved by repeating these subcycles two or three times, but in most cases there was little difference from using the raw HNC total correlation functions for the bridge function.

For the bulk electrolyte, the five dimensional quadrature for the first bridge diagram was carried out by expansion in Legendre polynomials.[21,25] For the wall ion–bridge function, Eq. (2.6) reduces to

$$D_\alpha(z_2)=2\pi^2\sum_{\gamma\lambda}\rho_\gamma\rho_\lambda\sum_{n=0}^{\infty}\left(\frac{2}{2n+1}\right)^2\int_0^{\infty}dr_3\, r_3^2\times\int_0^{\infty}dr_4\, r_4^2 h_{\alpha\gamma}(r_3)h_{\alpha\lambda}(r_4)\hat{h}_{\gamma\lambda}^{(n)}(r_3,r_4)\times\hat{H}_\gamma^{(n)}(z_2,r_3)\hat{H}_\lambda^{(n)}(z_2,r_4). \tag{2.15}$$

This result follows by rewriting Eq. (2.6) in a spherical coordinate system with the ion labeled 2 at the origin, (cf. Ref. 25). Here the Legendre coefficients of the bulk ion–ion total correlation function are

$$\hat{h}_{\gamma\lambda}^{(n)}(r,s)=\frac{2n+1}{2}\int_{-1}^{1}P_n(x)h_{\gamma\lambda}(\sqrt{r^2+s^2-2rsx})dx, \tag{2.16}$$

and those of the wall–ion total correlation function are

$$\hat{H}_\alpha^{(n)}(z,r)=\frac{2n+1}{2}\int_{-1}^{1}P_n(x)H_\alpha(z-rx)dx, \tag{2.17}$$

where $P_n(x)$ is the Legendre polynomial of order n. The discrete, orthogonal Legendre expansion of Attard[26] was used to evaluate the coefficients, and the contact discontinuities were treated analytically as described therein. [Note that the prefactor of $1-x_d$ should be eliminated from Eq. (A2) of Ref. 26.] By comparison, Ballone *et al.*[6] evaluated the first wall–ion bridge diagram by Monte Carlo quadrature.

The first wall–wall bridge function, Eq. (2.12), essentially reduces to a two dimensional integral when expressed in cylindrical coordinates, (the bulk correlation function can be integrated in the radial direction to give a function of $|z_3-z_4|$). This was evaluated directly, after some simplification using the fact that $H_\alpha(z)=-1$, $z<0$.

We solved the HNC and the HNCD equations for the bulk electrolyte using the usual method of fast Fourier transform of the Ornstein–Zernike equation.[21] The Coulomb potential for all of r was canceled in the direct correlation function before transformation; no adjustment was made at small r. Contact discontinuities in the correlation functions were transformed analytically, as has previously been described for hard-sphere fluids.[25] Typically, 2^{13} grid points were used, with a spacing such that the cutoff was around 10–100 Debye lengths. The bulk bridge functions were evaluated using typically 30 Legendre coefficients (and hence 30 angular nodes), 150 grid points for the remaining integrals, with a cutoff of 15 Debye lengths.

The wall–ion potential and density profiles were found in the HNC and HNCD approximations, using fast Fourier transformation to evaluate the fluid contribution to the Ornstein–Zernike convolution integral, (the constant wall contribution was evaluated directly before beginning the iteration procedure). The robust procedure of Badiali *et al.*,[27] as described by Ballone *et al.*,[6] was used to find the mean electrostatic potential corresponding to the current ionic profiles. Of the order of 2^{13} grid points were used, and the large z cutoff was generally around 20 Debye lengths. All integrals within the iteration loop were evaluated using the trapezoidal rule, using fast ($\mathcal{O}N$) algorithms. The wall–ion bridge functions were evaluated as described above, with similar numerical parameters to the bulk case. Little grid dependence was observed; there was reasonable agreement with Ballone *et al.*[6] in the case that they studied using Monte Carlo quadrature, although the present method appeared somewhat more accurate.

After convergence, typically six digits in the surface potential, the short-range part of the wall–ion direct correlation function was evaluated according to Eq. (2.9), and then the interaction free energy in the HNC and HNCD approximation was found, (using fast Fourier transformation of the Ornstein–Zernike convolution, and direct quadrature of the contributions from inside the wall). The same parameters as for the wall-ion calculations were used; the interaction free energy became unreliable for separations greater than about half the cutoff used for the wall–ion potential and density profiles. Typically 500 grid points and a cutoff of 10 Debye lengths were used for the wall–wall bridge function quadrature. The net pressure was obtained by a first order difference of the interaction free energy.

An idea of the computational burden of the singlet procedure can be obtained from the memory requirements. The bulk electrolyte HNC algorithm used about 2 Mbytes, the wall HNC algorithm used about 5 Mbytes, and the bridge function programs used about 2 Mbytes. No attempt was made to optimize the use of memory for the present benchmark calculations, and these values could be decreased by an order of magnitude in a practical situation. By comparison, a typical inhomogeneous integral equation calculation uses about 100 Mbytes.[26] The comparison of CPU requirements favors the singlet approach even further, mainly because of the availability of the fast Fourier transform. For simulations, the computational burden is in CPU time rather than memory. All of the results reported here were obtained interactively on a workstation.

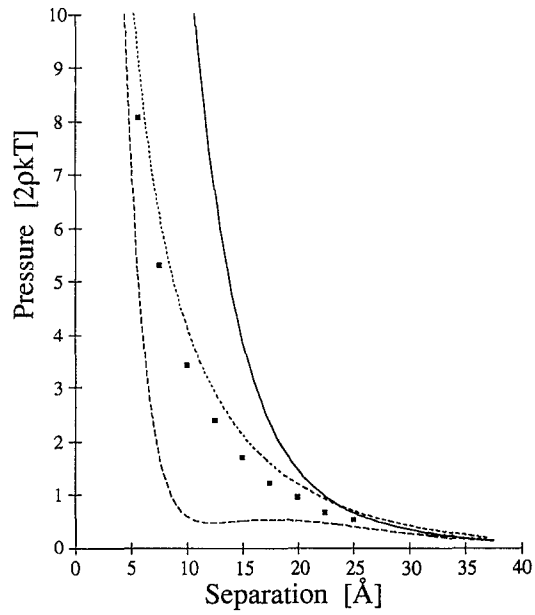

FIG. 1. The net pressure in 0.1 M monovalent electrolyte as a function of separation ($e/\sigma=250$ Å^2, $T=298$ K, $\epsilon=78.5$, $d=4.25$ Å). The symbols represent inhomogeneous HNC results (Ref. 28), the dotted curve is the nonlinear Poisson–Boltzmann approximation, and the dashed and the full curves are the present singlet HNC and HNCD theories, respectively. Here and in the remaining figures, the pressure is normalized by the total number density of the bulk electrolyte times the thermal energy, and the separation is the width of the interlayer accessible to the centers of the ions.

III. RESULTS

Results of singlet HNC and HNCD calculations will now be given for a restricted primitive model binary electrolyte ($q=q_+=-q_-$, $\rho=\rho_+=\rho_-$, $d=d_+=d_-$). Here the Debye screening length is given by $\kappa^2=2\beta q^2\rho/\epsilon_0\epsilon$, and the dimensionless surface charge is $s=\kappa\sigma/2\rho q$, with σ being arbitrarily chosen to be positive. Figures 1–4 are for monovalent electrolytes, and Figs. 5–10 are for divalents.

Figure 1 compares the pressure as a function of separation for 0.1 M monovalent electrolyte ($\kappa^{-1}=9.6$ Å), with one surface charge every 250 Å^2 ($s=3.5$). For separations beyond about 30 Å, (3 Debye lengths), the two singlet theories are in reasonable agreement with each other. At these separations the nonlinear Poisson–Boltzmann approximation overestimates the repulsion between the surfaces. If it were used to fit experimental data, then it would yield a lower effective surface charge than in reality. In contrast the singlet theories reliably estimate the attractive contributions to the pressure in this regime. The HNCD is close to the inhomogeneous HNC[28] at about 25 Å separation, but for smaller separations the first bridge diagram overcorrects the singlet HNC. (Data not shown indicates that this is usually the case in dilute electrolytes, and both are unreliable when the discrepancy between them becomes large.) The singlet HNC in the present figure remains repulsive over the whole regime, but shows a

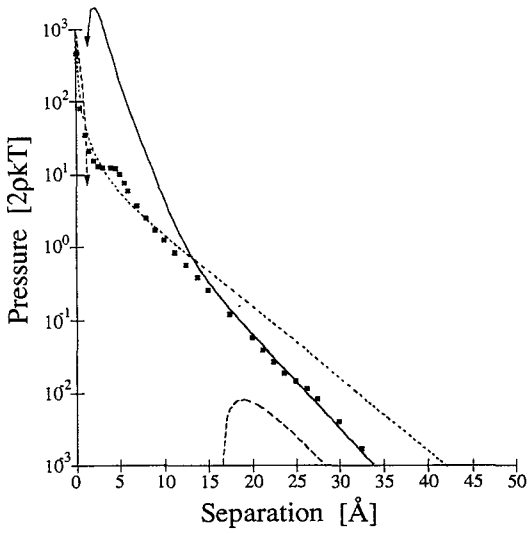

FIG. 2. The pressure in 0.5 M monovalent electrolyte ($e/\sigma=60$ Å^2, $T=298$ K, $\epsilon=78.5$, $d=4.6$ Å). The symbols represent inhomogeneous HNC results (Ref. 9) and the curves are as in the preceding figure. Attractions, which are not shown, are indicated by downward arrows.

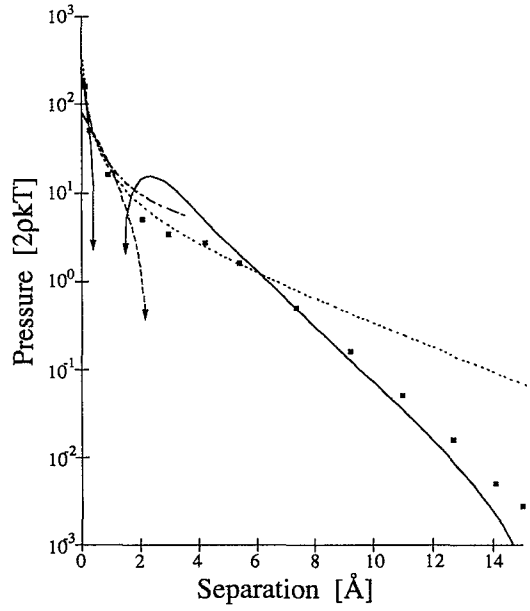

FIG. 3. Same as the preceding figure but in 1 M monovalent electrolyte and an area per unit surface charge of 85 Å^2, ($d=4.25$ Å). The dot–dash curve is the small separation limit, Eq. (3.1).

broad minimum in the pressure that is not present in the inhomogeneous calculations. This minimum will turn attractive as the surface charge is increased (e.g., at 60 Å^2 per unit surface charge in the same electrolyte, the singlet HNC turns attractive at a separation of 35 Å). The HNCD theory has a maximum in the pressure of 18.4 at 6.5 Å, and a minimum of -16 at 2.1 Å, which are not shown for clarity. Based on this and other data, it appears that at separations beyond 3 Debye lengths, the singlet theories are reliable for dimensionless surface charges less than about four.

Figure 2 shows the effect of increasing the concentration to 0.5 M ($\kappa^{-1}=4.3$ Å) and the surface charge to $|e/\sigma|=60$ Å^2, ($s=6.4$). The singlet HNC shows attractions between half and 3 Debye lengths, which are not present in the HNCD or in the inhomogeneous HNC[9] data. The plateau in the latter due to the ionic cores below about 10 Å separation has been exaggerated by the HNCD as it once again overcorrects the HNC. In this figure the HNCD appears quite accurate at large separations, giving the correct decay length, which is evidently not the Debye length, and it properly corrects the magnitude given by the singlet HNC. Because it has the incorrect decay length, the nonlinear Poisson–Boltzmann approximation increasingly overestimates the pressure at large separations, and is nearly an order of magnitude too large by 10 Debye lengths separation.

At the still higher concentration of 1 M (Fig. 3, $s=3.2$), the good performance of the HNCD beyond about 2 Debye lengths is again evident. The singlet HNC predicts attractions between 1 and 7 Debye lengths, and the HNCD gives a small attractive region at close separations. Again the HNCD has the correct asymptote; at very large separations, the HNCD begins to turn down beneath the inhomogeneous HNC data. We believe this to be an accurate effect that results from long-period oscillations in the bulk ionic correlation functions, which are reliably given by the HNCD.[20] Both simulations and inhomogeneous integral equations have difficulties at large separations, and Fig. 3 illustrates how the singlet approach complements them in this problematic regime.

In the limit of zero separation it is possible to obtain an exact expression for the pressure from the contact theorem and the electroneutrality condition. The latter states that the excess number of counterions must always balance the surface charge. Hence at zero separation the two-dimensional number density of the counterions is finite and nonzero, which implies that the three-dimensional number density must diverge like h^{-1}. The contact theorem states that the total pressure equals the contact density times the thermal energy. (The electrostatic terms, wall–wall and wall–ion, cancel.) The contact density equals the three-dimensional number density (i.e., the total number of ions divided by the volume), plus a correction linear in z, which is arbitrarily small because the separation is small. One concludes that

$$p(h)/2\rho k_B T \sim \frac{|\sigma|}{|e|\rho h} + \mathcal{O}(h^0), \quad h \to 0. \tag{3.1}$$

Only the divergent term has been retained in this expression. Contributions to the constant arise from the second term in the Taylor expansion of the density profile, from the counterions and co-ions present beyond that required by electroneutrality (their contribution to the pressure is bounded, see below), and from the bulk pressure, which is subtracted off the total pressure to give the net pressure. The last contribution may in many cases be the largest one. The Poisson–Boltzmann theory obeys this exact limiting

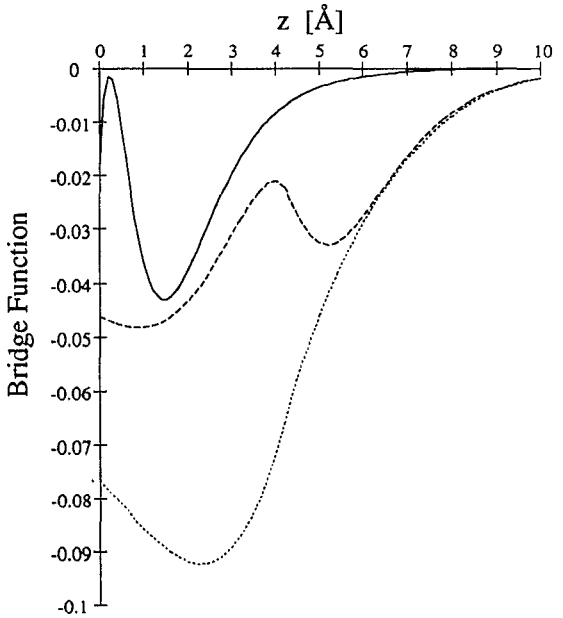

FIG. 4. Bridge functions for the case of Fig. 3. The solid curve is the wall–wall, multiplied by the area per unit surface charge, the dashed curve is the wall–co-ion, and the dotted curve is the wall–counterion.

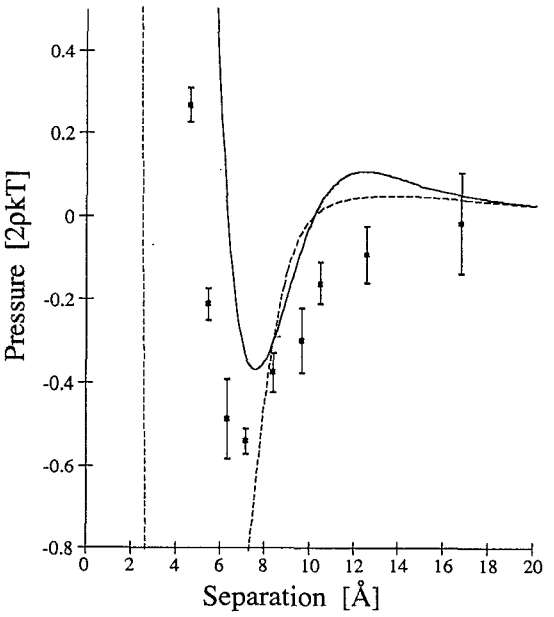

FIG. 5. The net pressure between charged surfaces in divalent 0.1655 M electrolyte with 176 Å^2 per unit surface charge. Here and in the remaining figures, $T=298$ K, $\epsilon=78.5$, $d=4.2$ Å. The symbols are simulation data (Ref. 11), the solid curve is the HNCD theory, and the dashed curve is the HNC.

law. The equivalent limiting expression for uncharged surfaces has been previously given;[29,30] in the present case, the net pressure is

$$p(h)/2\rho k_B T \sim \gamma_{\pm} - \phi + \mathcal{O}(h), \quad h \to 0, \tag{3.2}$$

where ϕ and $\gamma_{\pm}$ are the osmotic coefficient and the activity of the bulk electrolyte, respectively. This exact result resembles an ideal gas law because the two-dimensional number density vanishes for neutral surfaces, as discussed above.

The limiting result, Eq. (3.1), is shown at small separations in Fig. 3. It can be seen that all of the approximations show large repulsions at small separations, in qualitative agreement with the exact result. The HNC lies beneath the HNCD here, and appears to be approaching a finite value at contact.

Figure 4 shows the bridge functions calculated for the 1 M electrolyte with 85 Å^2 per unit surface charge. A negative value of the bridge function corresponds to a positive effective potential; the ordinate is effectively in units of the thermal energy per ion. Compared to the bare HNC result, the bridge function acts mainly to desorb the ions from the wall. The counterions find it unfavorable (compared to the bare HNC) to be about half a diameter from the wall. A similar observation holds for the co-ions, but for them there is minimal desorption at about one diameter from the wall. Qualitatively similar behavior for the wall–ion bridge functions has been reported by Ballone *et al.*[6] The wall–wall bridge function is mainly negative, and the direct effect on the bare HNC is to make the pressure between the walls beyond about 2 Å more repulsive (cf. Fig. 3). The direct effect of the wall–wall bridge function on the interaction free energy can be substantial; indirect effects due to using HNCD wall–ion correlation functions for the mean electrostatic potential and in the Ornstein–Zernike convolution integral appear as a perturbation in this case.

Figure 5 shows the pressure in 0.1655 M divalent electrolyte ($\kappa^{-1}=3.7$ Å, $s=3.8$), and it may be seen that both singlet theories are qualitatively correct. In the region of the minimum in the pressure, the HNC once more overestimates the attractions. Here the first bridge diagram provides the correct correction, and the HNCD theory can be regarded as quantitatively accurate. Of course, the nonlinear Poisson–Boltzmann theory does not give these attractions. The HNCD predicts a small maximum in the pressure at about 12 Å, which is not reflected in the grand canonical Monte Carlo data.[11] Not shown in the figure for the HNCD curve is another maximum of 10.4 at 2.6 Å, and a positive secondary minimum at 1.2 Å separation.

Figures 6–10 are for divalent electrolyte at the higher concentration of 0.971 M ($\kappa^{-1}=1.5$ Å). For the case of uncharged surfaces, Fig. 6, both the singlet theories underestimate the attraction, although the bridge functions in the HNCD approximation do bring the HNC results closer to the simulations. The singlet theories decay much more quickly than the simulation data. It is interesting to note that the pressure between uncharged surfaces is expected to decay with characteristic length $\kappa^{-1}/2$, at least at low coupling,[14,31,32] which is substantially quicker than the simulation data.[11] The 0.971 M divalent electrolyte has an activity coefficient of $\ln \gamma_{\pm} = -2.635$, and an osmotic coefficient of $\phi = p/2\rho k_B T = 0.605$,[32] or 0.651.[11] These lead to the exact limiting values for the net pressure, $p(0) = -0.533$, and -0.579, respectively, Eq. (3.2). The latter

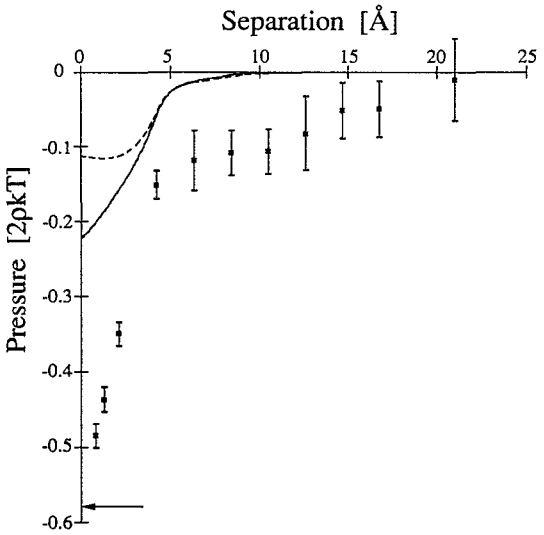

FIG. 6. Same as the preceding figure, but at a concentration of 0.971 M, and with zero surface charge. The arrow represents the limiting results, Eq. (3.2).

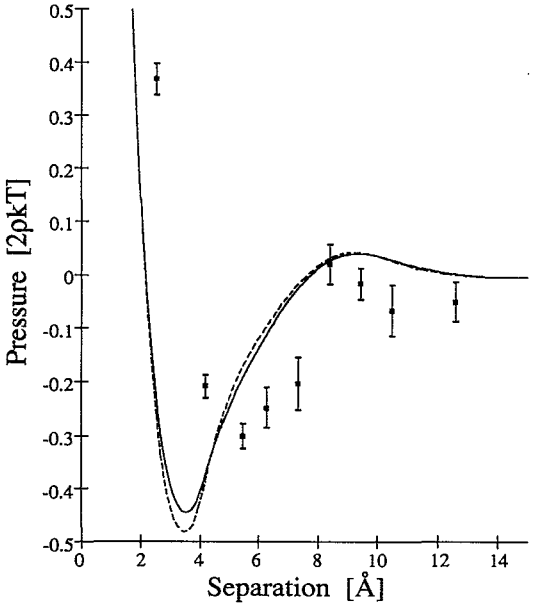

FIG. 8. Same as the preceding figure, but with a unit surface charge every 176 Å^2.

value is designated by an arrow in Fig. 8. The grand canonical simulations directly gave for the net pressure $p(0)/2\rho k_B T = -0.534$,[32] and -0.581 (extrapolated),[11] using their respective values for the bulk osmotic coefficient. The HNC prediction is -0.11, and the HNCD gives -0.23.

At the low surface charge of 1780 Å^2 in Fig. 7 ($s = 0.16$), there is better agreement with the simulations. In this case the value of the minimum pressure is relatively accurately given by the HNCD theory, which lies substantially closer to the simulations than the HNC result. Also shown in Fig. 7 is the small separation limit, Eq. (3.1), with the bulk osmotic coefficient subtracted. It can be seen that the simulation data is beginning to become repulsive at small separations, in accord with the limit, but that the singlet theories give a finite result at $h=0$. The large correction made to the HNC here by the first bridge diagram suggests that more diagrams are required in the series.

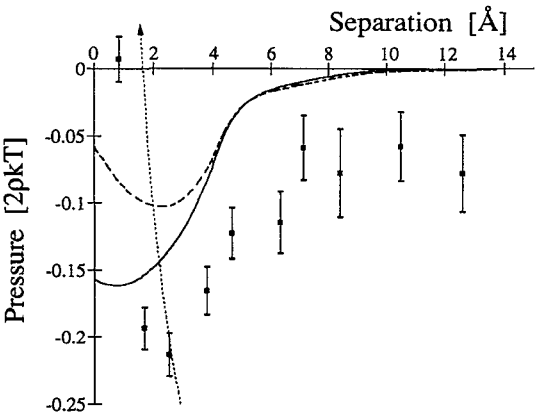

FIG. 7. As above, but with a unit surface charge every 1780 Å^2. The dotted curve is the analytic limiting result, Eq. (3.1), less the bulk osmotic coefficient.

Figure 8 shows the case of a moderate surface charge, 176 Å^2, ($s=1.6$), and it may be seen that the singlet theories are again qualitatively correct. Indeed, they appear relatively more accurate than in the case treated in Fig. 7. They both overestimate the minimum in the pressure, and locate it at about 4 Å rather than the 5.5 Å of the simulations. Both predict a maximum at about 9 Å, which can also be discerned in the simulation data.[11] It is somewhat surprising that the bridge functions give such a small correction to the HNC, much less than the discrepancy with the simulations. Compared to Fig. 5, (same surface charge, lower concentration and hence higher s), the HNC theory is here actually much better in the region of the minimum in the net pressure, and the first bridge diagram hardly makes any difference.

Figure 9 shows the pressure in the divalent electrolyte with one surface charge every 58.9 Å^2 ($s=4.7$). In addition to the singlet HNC result shown, two HNCD curves are given: for the dotted curve, HNC wall–ion total correlation functions were used to calculate the bridge functions, and for the full curve thrice-refined HNCD functions were used. This was the only case in which refinement made any significant difference. It can be seen that the bridge function substantially improves the HNC result, and that the process of refinement gives an important improvement to the HNCD theory in the region of the minimum in the pressure. The HNC theory accurately describes the maximum at about 8 Å separation, but overestimates the depth of the minumum in the pressure. The interesting structure in the HNC for separations in the range 5–14 Å has been smoothed by the inclusion of the bridge diagrams. This effect has been noted previously for a bulk Lennard-Jones fluid.[33] The HNCD theory remains quantitatively accurate in the region of the minimum in the pressure.

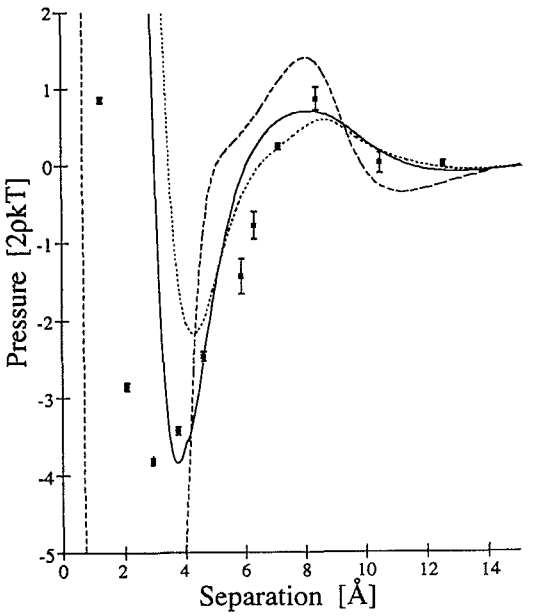

FIG. 9. Same as the preceding figure, but with a unit surface charge every 58.9 Å^2. The dashed curve is the HNC approximation, the dotted curve is the HNCD approximation, using HNC wall–ion total correlation functions for the bridge function, and the full curve is a self-consistent HNCD calculation.

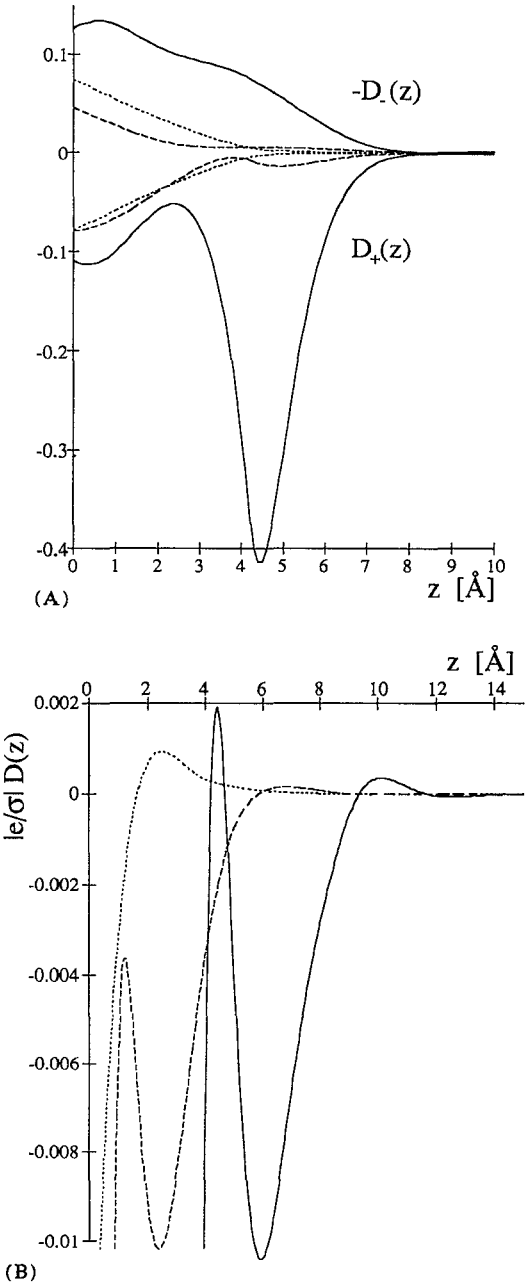

FIG. 10. Bridge functions in the 0.971 M divalent electrolyte. The solid, dashed, and dotted curves correspond to one surface charge every 58.9, 176, and 1780 Å^2, respectively. (A) Wall–co-ion, $D_+(z)$, and the negative of the wall–counterion, $-D_-(z)$. (B) Wall–wall, multiplied by the area per unit surface charge.

Bridge functions for three different surface charges are shown in Figs. 10. That the bridge function is mainly negative means that it effectively provides an extra repulsive potential. For the wall–ion bridge functions, Fig. 10(A), the two cases with the lowest surface charge show rather similar behavior, with the largest difference occurring for counterions. For the intermediate surface charge, the contact value for co-ions is -0.08, and for counterions it is -0.05, which tends to decrease the contact density of the ions compared to the bare HNC result. The wall–ion bridge functions for the largest surface charge, ($s=4.7$), are almost qualitatively different from the other cases shown. The co-ions have an effective depletion at about 4.5 Å separation of about half the thermal energy, whereas the counterions show a repulsion of about $k_BT/6$ at contact. Evidently the structure in the wall–ion bridge functions is mainly determined by hard-core effects, with the symmetry being broken by the charge on the ions.

The wall–wall bridge function is shown is Fig. 10(B) for the same three surface charges. Each curve has been multiplied by the area per surface charge to enable their structure to be seen on a common scale. [Note that it is the bridge function per unit area that is required in Eq. (2.14).] All three bridge functions are qualitatively the same, with a positive maximum and a negative minimum shown, but shifted in separation. Not shown is the primary minimum, which in order of increasing surface charge is -0.02, -0.3, and -11, occurring at contact in the first two cases, and at $z=0.65$ Å for the highest charge. Again the period of the oscillations appears related to the diameter of the ions.

The bridge function, whose short-range nature is apparent in these figures, is increasingly significant at short-separations, which is the reason that the HNC suffers at separations less than several Debye lengths. Similar comments hold for the higher order bridge diagrams that are not included in the HNCD. The bridge function (and to a lesser extent the Ornstein–Zernike series function) implicitly contains the effects of the wall on the inhomogeneous ion–ion correlations, even though the latter are not explicitly calculated in the present singlet approach. The bulk correlations are exponentially short-ranged, but the inhomogeneous ones decay as cubics parallel to the wall.[34,35] The former are the only ones that explicitly contribute in

the singlet approach; the slow decay of the latter remain implicit in the formally exact version of the present theory.

IV. CONCLUSION

The wall–wall Ornstein–Zernike equation has previously been derived for fluids with short-ranged potentials,[17] and here it was generalized to interacting charged surfaces in an electrolyte. What was sought was a tractable computational theory that included the effects of ion size and correlations, and the numerical results presented here show that in some regimes the singlet approach achieves this goal. The approximation appears reliable in the large-separation asymptotic regime. Also at higher concentrations, the oscillations in the pressure are reproduced at least qualitatively, and quantitatively in the case of high surface charges in divalent electrolyte. In other cases, noticeably for moderate to high surface charges in dilute monovalent electrolyte, the singlet approach is not as reliable as the nonlinear Poisson–Boltzmann.

The first (resummed) bridge diagram converted the HNC from a qualitative theory to a quantitative one. The influence of the bridge diagram on the ion profile at an isolated charged wall has previously been discussed,[6] and its efficacy here appeared even more marked for interacting electrical double layers. In some cases it overcorrected the HNC, which suggests that retaining the next term in the expansion could be worthwhile. This has previously been shown to be feasible for macrospheres in hard-sphere fluids,[25] and there is greater symmetry in the present planar geometry. An alternative likely improvement on the singlet wall–wall Ornstein–Zernike is the singlet dumbell Ornstein–Zernike of Lozada-Cassou.[15] Again the planar geometry would make the evaluation of the first (or even the next) bridge diagram feasible.

The present results suggest that the wall–wall procedure is relatively successful in the large separation asymptotic regime. This is perhaps expected, since the decay length, which is not the Debye length,[36] is determined by the bulk fluid,[20,37,38] for which the HNC is accurate. Also the amplitude is determined by the isolated-wall–fluid correlation functions,[20,37,38] and again the HNCD theory is known to be accurate for these.[6] As such, the singlet theory is probably a useful asymptotic complement to simulations and to inhomogeneous Ornstein–Zernike approaches, both of which are problematic in the large separation regime, and it may provide a useful point of departure for further analysis, as well providing a practical tool for the analysis of experimental data.

[1] S. L. Carnie and G. M. Torrie, Adv. Chem. Phys. **56**, 141 (1984).
[2] C. W. Outhwaite and L. B. Bhuiyan, J. Chem. Soc. Faraday Trans. 2 **79**, 707 (1983).
[3] M. Plischke and D. Henderson, J. Chem. Phys. **88**, 2712 (1988).
[4] G. M. Torrie and J. P. Valleau, J. Chem. Phys. **73**, 5807 (1980).
[5] D. Henderson, F. F. Abraham, and J. A. Barker, Mol. Phys. **31**, 1291 (1976).
[6] P. Ballone, G. Pastore, and M. P. Tosi, J. Chem. Phys. **85**, 2943 (1986).
[7] R. Kjellander and S. Marčelja, J. Chem. Phys. **82**, 2122 (1985).
[8] R. Kjellander and S. Marčelja, Chem. Phys. Lett. **127**, 402 (1986).
[9] R. Kjellander and S. Marčelja, J. Phys. (Paris) **49**, 1009 (1988).
[10] L. Guldbrand, Bo. Jönsson, H. Wennerström, and P. Linse, J. Chem. Phys. **80**, 2221 (1984).
[11] J. P. Valleau, R. Ivkov, and G. M. Torrie, J. Chem. Phys. **95**, 520 (1991).
[12] F. Oosawa, Biopolymers **6**, 1633 (1968).
[13] P. Attard, D. J. Mitchell, and B. W. Ninham, J. Chem. Phys. **88**, 4987 (1988).
[14] P. Attard, D. J. Mitchell, and B. W. Ninham, J. Chem. Phys. **89**, 4358 (1988).
[15] M. Lozada-Cassou, J. Chem. Phys. **80**, 3344 (1984).
[16] M. Lozada-Cassou and E. Díaz-Herrera, J. Chem. Phys. **92**, 1194 (1990).
[17] P. Attard, D. R. Bérard, C. P. Ursenbach, and G. N. Patey, Phys. Rev. A **44**, 8224 (1991).
[18] P. Attard and J. L. Parker, J. Phys. Chem. **96**, 10398 (1992).
[19] S. J. Miklavic and P. Attard, J. Phys. Chem. (submitted).
[20] P. Attard, Phys. Rev. E (submitted).
[21] R. Bacquet and P. J. Rossky, J. Chem. Phys. **79**, 1419 (1982).
[22] H. Iyetomi and S. Ichimaru, Phys. Rev. A **27**, 1241 (1983).
[23] D. Henderson, J. Chem. Phys. **97**, 1266 (1992).
[24] E. J. W. Verwey and J. Th. G. Overbeek, *Theory of the Stability of Lyophobic Colloids* (Elsevier, Amsterdam, 1948).
[25] P. Attard and G. N. Patey, J. Chem. Phys. **92**, 4970 (1990).
[26] P. Attard, J. Chem. Phys. **91**, 3072 (1989).
[27] J. P. Badiali, M. L. Rosinberg, D. Levesque, and J. J. Weiss, J. Phys. C **16**, 2183 (1983).
[28] S. Marčelja, Biophys. J. **61**, 1117 (1992).
[29] A. Luzar, D. Bratko, and L. Blum, J. Chem. Phys. **86**, 2955 (1987).
[30] D. Bratko, D. J. Henderson, and L. Blum, Phys. Rev. A **44**, 8235 (1991).
[31] B. Davies and B. W. Ninham, J. Chem. Phys. **56**, 5797 (1972).
[32] V. N. Gorelkin and V. P. Smilga, Sov. Phys. JETP **36**, 761 (1973).
[33] P. Attard, J. Chem. Phys. **95**, 4471 (1991).
[34] B. Jancovici, J. Stat. Phys. **28**, 43 (1982).
[35] S. L. Carnie and D. Y. Chan, Mol. Phys. **51**, 1047 (1984).
[36] D. J. Mitchell and B. W. Ninham, Chem. Phys. Lett. **53**, 397 (1978).
[37] P. Attard, C. P. Ursenbach, and G. N. Patey, Phys. Rev. A **45**, 7621 (1992).
[38] R. Kjellander and D. J. Mitchell, Chem. Phys. Lett. **200**, 76 (1992).